Ecological Applications, 28(6), 2018, pp. 1626–1639

From the stand scale to the landscape scale: predicting the spatial patterns of forest regeneration after disturbance

Kristen L. Shive,[1,6] Haiganoush K. Preisler,[2] Kevin R. Welch,[4] Hugh D. Safford,[3,4] Ramona J. Butz,[3,5] Kevin L. O'Hara,[1] and Scott L. Stephens[1]

[1]*Department of Environmental Science, Policy and Management, University of California, Berkeley, California 94703 USA*
[2]*USDA Forest Service, Pacific Southwest Research Station, Albany, California 94710 USA*
[3]*USDA Forest Service, Pacific Southwest Region, Vallejo, California 94592 USA*
[4]*Department of Environmental Science and Policy, University of California, Davis, California 95616 USA*
[5]*Department of Forestry and Wildland Resources, Humboldt State University, Arcata, California 95521 USA*

Abstract. Shifting disturbance regimes can have cascading effects on many ecosystems processes. This is particularly true when the scale of the disturbance no longer matches the regeneration strategy of the dominant vegetation. In the yellow pine and mixed conifer forests of California, over a century of fire exclusion and the warming climate are increasing the incidence and extent of stand-replacing wildfire; such changes in severity patterns are altering regeneration dynamics by dramatically increasing the distance from live tree seed sources. This has raised concerns about limitations to natural reforestation and the potential for conversion to non-forested vegetation types, which in turn has implications for shifts in many ecological processes and ecosystem services. We used a California region-wide data set with 1,848 plots across 24 wildfires in yellow pine and mixed conifer forests to build a spatially explicit habitat suitability model for forecasting postfire forest regeneration. To model the effect of seed availability, the critical initial biological filter for regeneration, we used a novel approach to predicting spatial patterns of seed availability by estimating annual seed production from existing basal area and burn severity maps. The probability of observing any conifer seedling in a 60-m^2 area (the field plot scale) was highly dependent on 30-yr average annual precipitation, burn severity, and seed availability. We then used this model to predict regeneration probabilities across the entire extent of a "new" fire (the 2014 King Fire), which highlights the spatial variability inherent in postfire regeneration patterns. Such forecasts of postfire regeneration patterns are of importance to land managers and conservationists interested in maintaining forest cover on the landscape. Our tool can also help anticipate shifts in ecosystem properties, supporting researchers interested in investigating questions surrounding alternative stable states, and the interaction of altered disturbance regimes and the changing climate.

Key words: community assembly; fire severity; forest regeneration; habitat suitability model; landscape ecology; spatial pattern; wildfire.

Introduction

The spatial pattern of an ecological disturbance can have significant consequences for many ecological processes and ecosystem services, including vegetation regeneration, hydrology, carbon storage, nutrient cycling, wildlife habitat, and susceptibility to future disturbance (Turner 1989). In forested ecosystems that are shaped by wildfire, the spatial pattern of fire severity, or the amount of tree mortality in a given area, can shape postfire vegetation regeneration patterns. In turn, these patterns shape longer-term demographic processes and community trajectories (Turner et al. 1997). Spatial patterns of severity are particularly important in forests where the foundation species lack serotiny, long-lived soil seed banks, or sprouting ability, because regeneration patterns will be dependent on the spatial configuration of live, remnant individuals to provide a seed source (Haire and McGarigal 2010, Crotteau et al. 2013, Dodson and Root 2013, Chambers et al. 2016, Donato et al. 2016, Harvey et al. 2016, Welch et al. 2016).

Manuscript received 13 February 2018; revised 18 April 2018; accepted 27 April 2018; final version received 22 May 2018. Corresponding Editor: John B. Bradford.
[6] E-mail: shive.kristen.l@gmail.com

Understanding the relationship between the spatial patterns of fire severity and postfire regeneration processes across the landscape is critical in the face of changing fire regimes. Shifts in the spatial patterns of severity could have significant effects on postfire forest regeneration if the scale and severity of the disturbance no longer match the regeneration traits of the dominant species (Collins et al. 2017, Stevens et al. 2017). A prominent example of this potential disconnect is in many of the semiarid conifer forests of the western United States, where the historical fire regime created a heterogeneous landscape that was characterized by frequent, low-to-moderate severity fires with smaller patches of high severity where all or nearly all trees are killed (Parsons and DeBenedetti 1979, Stephens and Collins 2004, Collins et al. 2009, Collins and Stephens 2010, Perry et al. 2011). This heterogeneity provided a diversity of habitats across space and also likely enabled the persistence of the foundation conifer species through time by generally limiting the distance between live tree seed sources after disturbance. Over the last century, fire exclusion in western semiarid conifer forests and high-grade logging of large trees in many areas have led to increases in fuels, forest density, and the component of fire-intolerant species (Stephens and Ruth 2005, Sugihara et al. 2006, Safford and Stevens 2017).

As a result, modern fires tend to burn through a more homogeneous forest with a more continuous fuel bed than they did prior to Euro-American settlement (Collins et al. 2011). In concert with the warming climate, these conditions have led to more severe fires with increased high-severity patch sizes in some forested areas (Westerling et al. 2006, Miller and Safford 2012, Miller et al. 2012); today, high-severity patches of thousands of hectares are not uncommon. By increasing the distance to live trees, the increase in high-severity patch size may result in limited reforestation and potential shifts to non-forested vegetation types, which can be maintained by positive feedbacks with recurrent fire (Coppoletta et al. 2016, Tepley et al. 2017). A better understanding of the relationship between severity patterns and regeneration processes in these ecosystems can help anticipate potential shifts in vegetation type and structure, and how such shifts may affect ecological processes and ecosystem services (Turner et al. 2013).

In addition to seed source proximity, postfire conifer establishment is also modified by other biotic and abiotic drivers that vary spatially across the landscape. Other biotic drivers of conifer tree regeneration patterns include competition (Dodson and Root 2013), facilitation (Keyes et al. 2009), herbivory (Vander Wall 2008), and local stand structure and species traits (Dobrowski et al. 2015). Broader scale abiotic drivers include topography and climate, where climate parameters for the regeneration niche are distinct from those occupied by mature trees (Dobrowski et al. 2015); fine-scale variations in abiotic conditions, including microclimates, are also critical for conifer establishment (Gray et al. 2005, Puhlick et al. 2012, Dobrowski et al. 2015). Understanding the relative importance of remnant seed tree spatial patterns to these other drivers can bolster our understanding of community assembly after landscape-scale disturbance. Moreover, it can improve spatially explicit predictions of postfire conifer regeneration that can be used to support land management and conservation planning.

To better understand the relationship between spatial patterns of burn severity and regeneration processes in non-serotinous conifer forests, we used data from 1,848 plots in 24 wildfires that burned in mixed conifer and yellow pine forests throughout California to build a habitat suitability model for postfire conifer regeneration. Recent work using data from 14 of these fires identified proximity to seed source as a primary driver (Welch et al. 2016); here, we build on that work by more closely examining the importance of spatial patterns relative to other drivers of postfire conifer regeneration, with the goal of scaling these findings from the plot scale to the landscape scale so that they can be used to forecast regeneration patterns on new fire events. This approach produces prediction maps that can be generated immediately postfire to help land managers with postfire management decision making. Depending on management goals, these maps could support decisions on where to plant trees if rapid reforestation is desired, especially where resources are limited. More broadly, these maps can also inform questions about ecological change after disturbance under altered fire regimes.

Our ability to effectively scale these plot data to an entire fire event or across a landscape is necessarily limited to the data that are available at those scales. Data on broad-scale abiotic drivers, such as topography and climate, are widely available; however, data on fine-scale biotic drivers, such as competing vegetation, herbivory, microclimates, and distance to individual seed trees, are generally not. Several authors have used Euclidean distance to the nearest "lesser burned" edge as a proxy for field-measured distance to individual seed sources in high-severity areas (where lesser burned edge refers to areas of lower burn severity where at least some seed trees survived) (Bonnet et al. 2005, Chambers et al. 2016, Harvey et al. 2016). This seed availability proxy (SAP) has helped to explain regeneration patterns where field data on distance to seed tree are lacking; however, this approach does not fully incorporate the importance of high-severity patch size and configuration. It is possible to have two sampling locations with equal Euclidean distance to lesser burned edge, but that are situated in otherwise very different patch sizes and shapes, which may in turn influence the total seed availability at each plot.

Our goal was to improve on this SAP using techniques to better model seed availability by incorporating neighborhood effects. Using maps of estimated basal from the Landscape Ecology, Modeling, Mapping and Analysis (LEMMA) Lab, a collaborative research group at the US Forest Service (USFS) Pacific Northwest Research Station and Oregon State University (Ohlmann and Gregory 2002), we created maps of estimated postfire annual seed production and then smoothed these surfaces to simulate a neighborhood effect. We created a suite of these SAPs with a range of neighborhood smoothing distances, from 50 to 500 m in 50 m increments, to better understand the best neighborhood size for predicting the probability of conifer regeneration.

We then combined the SAP approach with climatic, topographic, and burn severity data to examine the relative importance of the spatial patterns of seed availability to these other drivers and to also predict the spatial pattern of postfire conifer regeneration after future fires. Specifically, we asked (1) What environmental variables are most important for forecasting postfire conifer regeneration? (2) How can we best scale plot-level relationships to the scale of the landscape with seed availability proxies? (3) How do forecast models with seed availability proxies compare with field-based models that include variables for competition and individual seed sources?

Methods

Study sites

We used a region-wide monitoring data set collected by the USFS Region 5 Ecology Program and partners at the University of California-Davis (Welch et al. 2016) and Humboldt State University (DeSiervo et al. 2015). A total of 1,848 plots were installed in 24 wildfires throughout California (Fig. 1) that burned between 1999 and 2013. Plots were measured between 1 and 12 yr postfire, with most measured 5 yr after fire (Table 1). Plots were installed between 1,000 m and 2,500 m in elevation, across a range of forest types that were conifer-dominated prefire, with an emphasis on forest types that included a substantial component of the following species' of interest: ponderosa pine (*Pinus ponderosa* Lawson & C. Lawson), sugar pine (*Pinus lambertiana*

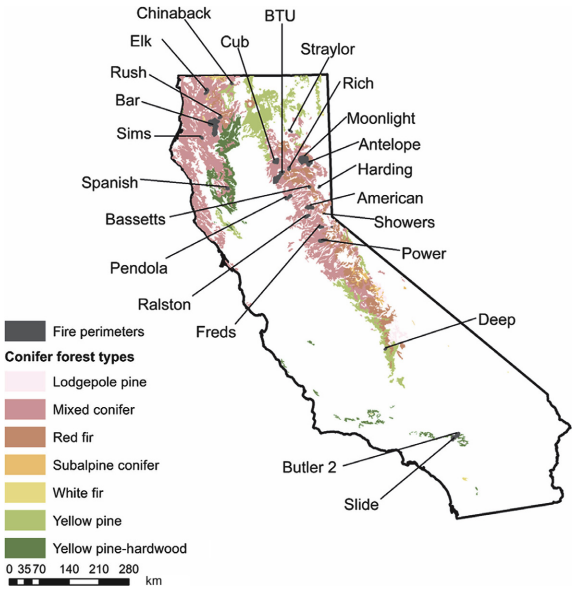

FIG. 1. Locations of all fires where plots were measured across the state of California. Forest types were derived from California Wildlife Habitat Relationship (WHR) Types, acquired from the USFS Pacific Southwest Region Geospatial Data website (https://www.fs.usda.gov/main/r5/landmanagement/gis). Fire perimeters were buffered by 2 km to increase visibility in the figure.

Douglas), Jeffrey pine (*Pinus jeffreyi* Grev. & Balf.), white fir (*Abies concolor* (Gordon & Glend.) Hildebr.), incense-cedar (*Calocedrus decurrens* (Torr.) Florin), and Pacific Douglas-fir (*Pseudotsuga menziesii* (Mirb.) Franco var. *menziesii*). Less than 10% of plots were located in areas with notable components of red fir (*Abies magnifica* A. Murray bis), lodgepole pine (*Pinus contorta* Louden ssp. *murrayana* (Grev. & Balf.) Critchf.), western white pine (*Pinus monticola* Douglas), or knobcone pine (*Pinus attenuata* Lemm.). The forests we studied fall primarily into the general "yellow pine-mixed conifer" category described by Safford and Stevens (2017). For each fire, plots were located at the vertices of a 200-m grid overlaid across the fire severity map in ArcMap 10.4 (ESRI, Redlands, California, USA). Continuous burn severity imagery was obtained from USFS Region 5 (data *available online*).[7] Burn severity maps were generated from 30 m pixel Landsat imagery, using the Relativized differenced Normalized Burn Ratio (RdNBR; Miller and Thode 2007). RdNBR is derived by calculating the Normalized Burn Ratio (NBR) that is sensitive to chlorophyll and moisture (using the near- and mid-infrared, Landsat bands 4 and 7) for both pre- and postfire imagery, which are then differenced (dNBR) and relativized (RdNBR) to account for variation in prefire cover. Of the 1,848 plots, 40% were located in high-severity areas with >90% overstory mortality, 29% were located in moderate-severity areas that range from 25 to 90% mortality, 20% were located in low severity areas with <25% mortality, and the remaining 10% of plots in unburned areas. One exception to this design was the 2013 Rim Fire, where the same field data collection protocol was used, but the methods for randomizing the plot locations differed. There plots were co-located with a wildlife study and study on mulch effects on vegetation (Shive et al. 2017); only unmulched control plots were included in this analysis. For all fires, areas with intensive postfire management, such as salvage logging and planting, were excluded from analysis. We did not attempt to control for prefire treatments.

Field data collection

Regeneration data were recorded in 60-m^2 plots. Regeneration of conifer seedlings <1.37 m tall was tallied by species and age; age was determined by counting bud scars (i.e., branch whorls). Our own field assays and other published work suggest that seedlings <7 yr old can be relatively accurately aged using bud scars (~65–80% absolute accuracy with mean errors generally <0.25 yr over the range 0–7 yr (Daly and Shankman 1985, Millar et al. 2004, Urza and Sibold 2013; H. D. Safford, *unpublished data*). Crews made ocular estimates of cover by life-form (tree, shrub, forb, and graminoid) and ground cover (litter, rock, wood, and bare soil). Live overstory tree basal area was collected by species using variable radius plots, using basal area gauges with basal area factors that ranged from 5 to 40, depending on site characteristics (Avery and Burkhard 2015). Finally, distance to potential seed source was recorded for all focal conifer species that were visible from the plot using a laser range finder. Potential seed sources were live trees that were bearing cones or had borne cones in the previous year.

Remote sensing products

We used digital elevation models (DEMs) with a 10-m resolution acquired from the USGS (U.S. Geological Survey 2014) and generated slope and aspect from the DEM using ESRI ArcMap 10.4. We downloaded 270-m resolution raster data sets of 30-yr climate averages (1981–2010) for climatic water deficit (CWD; mm), annual precipitation (PPT; mm), actual evapotranspiration (AET; mm), 1 April snow water equivalent (Snowpack; mm), and minimum temperature (TMIN; °C) from the California Climate Commons (data *available online*).[8] These climate averages were modeled using the basin characterization model (Flint et al. 2013). We extracted all of these data to each sampling plot (Table 2).

For burn severity, we assigned the raw RdNBR values for both the Initial Assessments (IAs), which were created immediately postfire, and the Extended Assessments (EAs), which were created approximately one year postfire, to each regeneration plot. Because IAs were not available for four wildfires (Freds, Pendola, Power, Spanish), we created a model to predict IA values from EAs, using the remaining 18 fires in a simple linear regression model that included both EA and its squared term to estimate a nonlinear relationship (adjusted $r^2 = 0.728$). To compare the relative performance of the EA and IA values, we used the Akaike information criterion (AIC). AIC is the log-likelihood of the model (a measure of overall model fit) adjusted for the number of parameters in the model. The IA performed much better than the EA when tested against regeneration probability independently (AIC: 1,926.68 and 1,973.27, respectively) and so was used in all models.

[7] http://www.fs.usda.gov/main/r5/landmanagement/gis

[8] http://climate.calcommons.org/

TABLE 1. List of wildfires used in analysis.

Fire name	Fire year	Time postfire measured (yr)	National forest	Size (ha)	No. plots
American River Complex	2008	5	Tahoe	8,480	78
Antelope	2007	5	Plumas	9,351	91
Bar	2006	5	Shasta-Trinity, Klamath	40,858	84
Bassets	2006	5	Tahoe	939	79
BTU Lightning	2008	5	Plumas	21,340	95
Butler 2	2007	5	San Bernardino	5,980	56
Chinaback Complex	2007	5	Klamath	1,280	72
Cub Complex	2008	5	Lassen	8,406	118
Deep	2004	5	Sequoia	1,364	23
Elk Complex	2007	5	Klamath	5,747	49
Freds	2004	5,7,8	Eldorado	3,298	44,6,6
Harding	2005	5	Tahoe	954	73
Moonlight	2007	5	Plumas	26,595	118
Pendola	1999	11,12	Tahoe	4,752	33,47
Power	2004	5	Eldorado	6,987	106
Ralston	2006	5	Eldorado, Tahoe	3,227	74
Rich	2008	3,4	Plumas	2,703	74,37
Rim	2013	1,2	Stanislaus	104,131	53,41
Rush	2006	5	Klamath	2,021	55
Showers	2002	7	Lake Tahoe Basin Management Unit	129	10
Sims	2004	6,9	Shasta-Trinity, Six Rivers	1,541	68,10
Slide	2007	5	San Bernardino	5,208	52
Spanish	2003	7	Mendocino	2,584	158
Straylor	2004	5	Lassen	1,413	40

Note: For fires measured over multiple years, plot counts per year are listed in the same sequence as the number of years postfire measured.

TABLE 2. Candidate variables for the forecast model and field-derived variables used in the full model.

Variable	Units
Climatic	
Actual evapotranspiration	mm
Annual precipitation	mm
Climatic water deficit	mm
Minimum temperature	°C
Snow water equivalent, 1 April	mm
Topographic	
Elevation	m
Aspect	degrees
Slope	%
Seed availability proxies (SAPs)	
Kernel surface of seed availability at 10 bandwidths (50–500 m)	
Euclidean distance to unburned, low, or moderate severity edge	
Burn severity	
Initial assessment (RdNBR)	
Field-derived	
Shrub cover	%
Litter cover	%
Live tree basal area	m^2/ha
Distance to live tree seed source	m

Note: RdNBR, Relativized differenced Normalized Burn Ratio.

We obtained maps of estimated basal area by species from gradient nearest neighbor structure (species-size) maps produced by the Landscape Ecology, Modeling, Mapping and Analysis (LEMMA) Lab, a collaborative research group at the USFS Pacific Northwest Research Station and Oregon State University (Ohlmann and Gregory 2002). These maps estimate basal area by species at the 30-m pixel scale that are based on nearest-neighbor relationships between remotely sensed Landsat data and USFS Forest Inventory and Analysis (FIA) plots. Kappa coefficients, which measure intragroup agreement for categorical calculations, for our species of interest were as follows: Douglas-fir (0.5644), incense-cedar (0.5093), Jeffrey pine (0.4362), ponderosa pine (0.5018), sugar pine (0.4176), white fir (0.5465; Ohmann et al. 2014). Because the LEMMA product was generated in 2012 (Ohmann et al. 2014), it reflected postfire forest structure on all fires except for the Rim Fire; we reduced the basal area estimates in the Rim Fire using burn severity maps. This involved classifying the burn severity maps into seven classes of percentage of basal area mortality (0%, 1–10%, 10–25%, 25–50%, 50–75%, 75–90%, 90–100%) as modeled by Miller et al. (2009), and multiplying the LEMMA basal area estimate by the midpoint for each class. For the highest severity class (90–100% basal area mortality), we used 100% rather than the midpoint (95%) because it was more representative of that class in the Rim Fire (data from the Rim Fire documented 99.5% basal area loss in the highest severity category; K. Shive, *unpublished data*). In addition, other work in the Rim Fire showed that basal area loss in the highest severity class was >95% for most plots (Lydersen et al. 2016).

Creating seed availability proxies (SAPs)

Euclidean distance.—We measured the shortest distance from each sampling point to the nearest, lesser burned edge (pixels categorized as unburned, low or moderate severity in

the classified burn severity map). For plots located in non-high-severity pixels, distance was set to zero. We used the Near tool in ArcMap 10.4 to measure distances.

LEMMA based.—To estimate relative seed production across the landscape, we calculated annual seed production from basal area as modeled by LEMMA (Ohmann et al. 2014). We calculated species-specific annual seed production for each 30-m pixel (number of seeds per 900 m^2) using established equations based on seed mass by species and basal area (Greene and Johnson 1994). These equations reflect established relationships that generally describe increases in the number of seeds produced with increasing tree crown size within a given species, but overall lower numbers of seeds produced for heavier seeded species relative to lighter seeded species (Venable 1992). To calculate seed production, we converted basal area to leaf mass (Greene and Johnson 1994: Eq. 2) and then estimated seed production based on leaf mass and individual seed mass (Greene and Johnson 1994: Eq. 5). We calculated seed mass by species from the average number of seeds per pound (Franklin and Schopmeyer 1974, Krugman and Jenkinson 1974, Owston and Stein 1974, Stein 1974, USDA Forest Service 1990). The equations provided in Greene and Johnson (1994) were intended for use with basal area of individual trees, but because we lack detailed stand structure data, we used total basal area by species for each pixel as an estimate of the relative magnitude of seed production across the landscape. We then summed the number of seeds produced by each of the focal species for each pixel.

We converted each burn severity pixel to a 30-m point grid across each fire perimeter with a 500 m buffer. Total estimated annual seed production was assigned to each point, which was used to create smoothed surfaces of seed availability using Gaussian density kernels centered at each point. Seed dispersal curves are generally modeled with fat-tailed exponential or lognormal curves (Clark et al. 1999, Greene and Johnson 2000), but these were not available for landscape-level modeling in ArcMap 10.4. We created these smoothed surfaces using a range of bandwidths (or radii) from 50 m to 500 m at 50-m intervals (Fig. 2c–e). Since all of the bandwidths are greater than the distance between points, this creates a contiguous surface of overlapping kernels with variable density values, in this case seed production (Fig. 2e). The Kernel Interpolation Tool with Barriers in ArcMap 10.4 was used to develop the smooth surfaces.

Statistical models

We used generalized additive models (GAMs; Hastie et al. 2001) to build binomial models for predicting the probability of conifer regeneration, lumping our six species of interest (Douglas-fir, incense-cedar, Jeffrey pine, ponderosa pine, sugar pine, white fir) into a single presence/absence variable. Because we were building these models to forecast regeneration across an entire fire, including on future wildfires, we examined only variables that could be predicted after a fire and therefore available for use in a forecasting framework; hereafter, we refer to these models as "forecast" models. We examined a suite of potential climatic, topographic, burn severity, and SAP variables (Table 2) to build a forecast model that predicts the probability of observing at least one regenerating conifer in a 60-m^2 area, which is the area of field plots used to build the model. We also included time since fire as the number of years after the fire that the measurements were taken.

To find the best forecast models, we compared candidate models including burn severity (IA) and all climatic and topographic variables other than a SAP term, and dropped non-significant terms one at a time; however, since several of the climate variables were correlated, we also checked for changes in AIC with and without these terms. Further model examinations included visual inspections of partial residual plots as well as *P* values for relevant variables. The partial residual plots show the magnitude of change in the odds of regeneration, relative to the odds at the variable's mean, which is set to 1. The partial residuals plot for each variable represents the expected change in the odds of the response while controlling for all other variables in the model. We also included the individual fire as a random effect to account for differences between fires that we were unable to measure in the field. Once we determined the best predictor variables other than a SAP term, we then used them in a base model and compared models with SAPs at different scales (50–500 m) to determine the most important neighborhood of seed availability for predicting regeneration with AIC. All analyses were performed using the mgcv package in R (Wood 2006).

To better understand how well the kernel-based SAPs helped predict regeneration relative to other methods, we then compared the best forecast model with models where we substituted the kernel-based SAP with (1) no SAP, (2) the Euclidean distance to nearest, lesser burned edge SAP, and (3) field-derived distance to seed tree. This comparison held the rest of the model constant, enabling the evaluation of the SAP itself. Next, we also wanted to better understand how much information is lost when using the limited number of variables available for prediction (Table 2) at the landscape scale after a new wildfire. In the forecasting framework, spatially and temporally variable responses such as regenerating shrub cover cannot be readily predicted across the landscape, yet we know these are important drivers of postfire conifer regeneration (Collins and Roller 2013, Welch et al. 2016). To evaluate how our forecast model performed in comparison with models with these important, local-scale drivers, we compared our forecast model to a "full" model with field-derived variables that were determined to be significant on a subset of our fires by Welch et al. (2016); specifically, this included variables that represented competition (shrub cover), microsites (litter cover), and seed sources (distance to individual live trees). We compared these models with AIC values as well as visual assessments of the model fitted values relative to actual observations (Fig. 4).

Model validation and predictive map

To account for variability between fires, and to mimic forecasting a future fire based on past fires, we used the leave-one-out method of model cross-validation, leaving each fire out of the model and predicting it with a model from the remaining 23 fires (Hastie et al. 2001). Using the predictions from the cross-validation procedure, we created a reliability diagram by binning these predictions into the following seedling presence probability classes: 0–0.2, 0.2–0.4, 0.4–0.6,

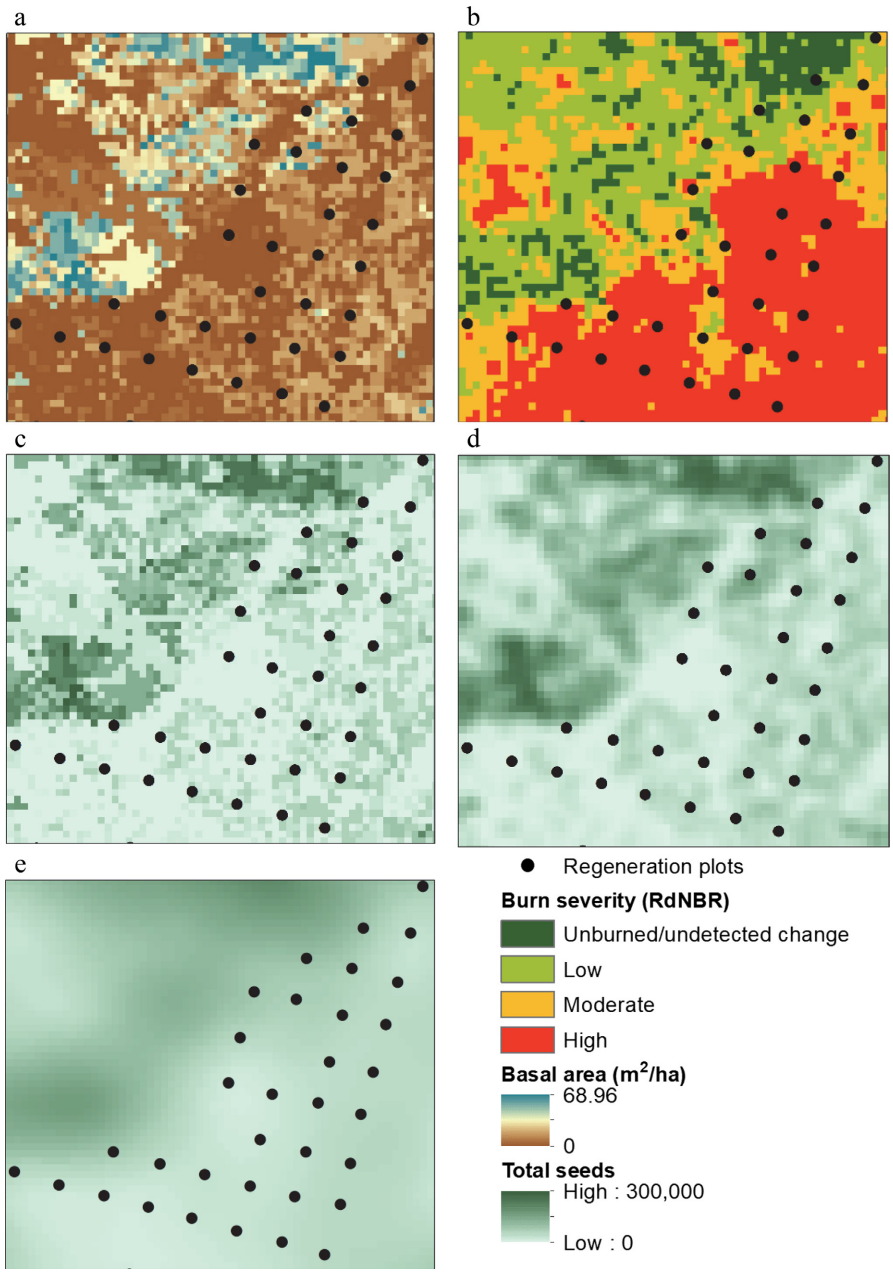

FIG. 2. Work flow for creating kernel surface as a proxy of relative seed availability. This involved confirming that (a) the LEMMA basal area estimates generally matched (b) the burn severity imagery to ensure the LEMMA reflected postfire patterns. Basal area was converted to (c) annual seed production and smoothed using a kernel surface; surfaces generated from a (d) 50-m and (e) 250-m bandwidth are shown here. The black dots represent field sampling plots.

0.6–0.8, and 0.8–1.0. Within each category, we calculated the frequency of observed positive cases (conifers present) in the total number of observations in that category for each fire, excluding instances where the number of observations for an individual fire within a class was <5. We then created boxplots with the probability classes on the *x*-axis and observed frequency of positive cases per fire per class on the *y*-axis, as a means to show the expected variability in prediction values.

To create an example of a regeneration probability predictive map, we converted the burn severity raster to a point grid on a "new" fire (the 2014 King Fire) and created the relevant SAP using the 2012 LEMMA basal area estimates, adjusted by the basal area mortality classes from RdNBR (described above for the Rim Fire). We then overlaid all relevant climatic and topographic variables and assigned values to each point in the point grid. Using the forecast model with all fires included, we then predicted the probability of conifer regeneration in a 60-m^2 area for each point in the grid. To show the inherent variability in the model, we binned the point predictions into the same classes used for the reliability diagram and converted them to a raster, which was color-coded to match boxplots from the reliability diagram. We also included boxplots and a summary table of the observed conifer seedling density data for each class.

Results

The best model for forecasting the odds of conifer regeneration included annual precipitation, climatic water deficit, actual evapotranspiration, snowpack, aspect, slope, number of years postfire, burn severity, and the kernel-based SAP with a 150-m neighborhood. Annual precipitation and continuous burn severity (IA) had the largest effect on the odds of regeneration, demonstrated by their percentage of total chi square values (22.0% and 21.8%, respectively) (Fig. 3). The odds of regeneration in a 60-m^2 area were roughly seven times greater at precipitation levels greater than 2,000 mm than at locations with average precipitation (~1,200 mm). Burn severity (IA) had strong negative effects on regeneration at RdNBR values above about 700, which corresponds to high severity. At sites that experienced very high burn severity (RdNBR >1000), the odds of regeneration were ~60% less than sites with moderate-to-low burn severity (<500). Increasing estimated annual seed input generated from the 150 m neighborhood kernel surface strongly increased the odds of regeneration, but the percentage of total chi square was low (6.5%). However, this variable was moderately correlated (Pearson's: −0.48) with burn severity, which can affect chi square and *P* value estimates. An exploratory model without the correlated burn severity (IA) variable increased the kernel-based SAP percentage of chi square to 39%, and a model without the kernel-based SAP increased the burn severity (IA) percentage of chi square to 35%; the overall shape of the responses did not change when these variables were included alone. In both cases, they were at least 10% higher in terms of percentage of chi square than any other variable in the model, including annual precipitation, suggesting that these two variables together are the most important drivers of regeneration. Aspect explained

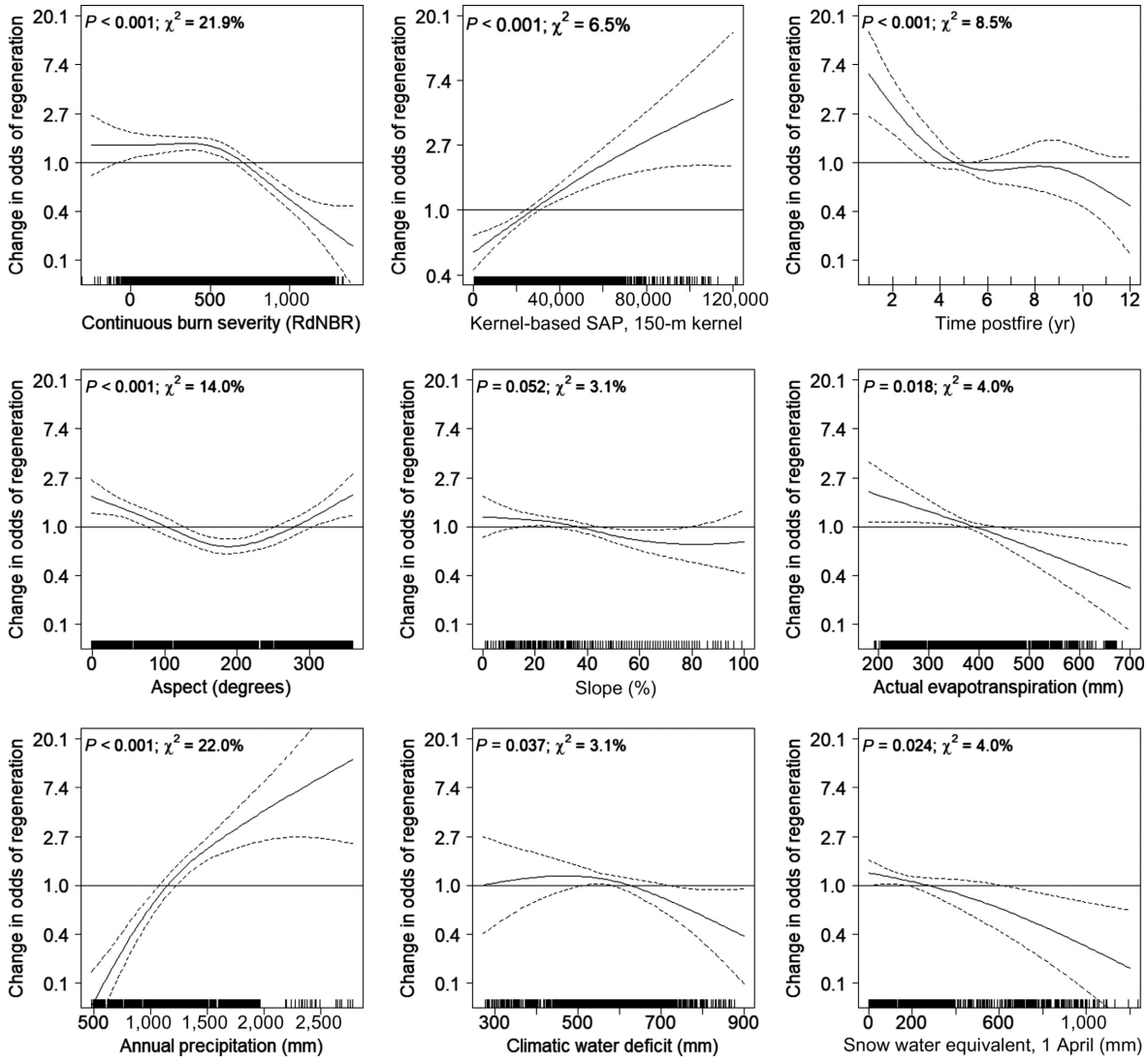

Fig. 3. Partial residual plots for model predicting seedling presence/absence of any of the six conifer species of interest. Residual plots show how each variable (*x*-axis) influences the probability of conifer regeneration in a 60-m^2 area (*y*-axis, log scale), given that all other variables are in the model. The response at the variable's mean is set to one on the *y*-axis; deviations from one are the magnitude of change in the log odds of observing regeneration. *P* values and the percentage of chi square attributed to each of these predictors are in the upper left corner. SAP, seed-availability proxy.

14% of the variation, where north- and east-facing aspects had a positive effect on the odds of regeneration. The estimated odds of regeneration declined through time, with the highest probabilities predicted for fires measured in the first few years postfire. The remaining explanatory variables included in the model improved model fit as assessed by AIC and the reliability diagrams, but had percentage of chi square values <5%. Increasing slope, AET, CWD, and snowpack values all had a generally weak, negative effect on the odds of regeneration (Fig. 3). All climate variables were moderately correlated (with Pearson's coefficients ranging from 0.49 to 0.66), so we also examined models with all other variables and individual climate variables one at a time, since the inclusion of correlated variables can affect the estimation of chi square and *P* values. In the absence of the other correlated variables, none of the variables differed dramatically from the model with all climate variables in terms of model estimates or the partial residuals shown in Fig. 3. Minimum temperature and elevation were not significant, and models with and without either variable did not differ in terms of AIC and so both were eliminated from the final model. All reports of variable relationships with estimated odds of regeneration are made with all other variables in the model.

The forecast model with Euclidean distance ($P = 0.037$; AIC = 2,046.01) was only slightly better than a model with no SAP term (AIC = 2,049.62). The best neighborhood size for the kernel-based SAP was 150 m ($P < 0.001$; AIC = 2,024.85). However, SAP neighborhoods of 200 m and 250 m all had dAIC < 2, suggesting no real difference between these neighborhood sizes. Not surprisingly, field-measured locations of nearest potential seed tree performed the best ($P < 0.001$; AIC = 1,983.51). The full model that included field-derived data on shrub cover ($P < 0.001$), litter cover ($P = 0.017$), live tree basal area ($P = 0.110$), and distance to individual seed tree ($P < 0.001$) performed substantially better (AIC = 1,956.80) than any forecast model. Differences between these models in terms of estimated probabilities versus actual observed frequencies are shown in Fig. 4; the figure shows estimated probabilities by presence versus absence to show how well the models are correctly predicting regeneration presence as well as where it may be overpredicting regeneration where it is actually absent.

Model validation and forecasting

The leave-one-out cross-validation procedure showed good agreement between the predicted classes and empirical distributions of regeneration frequencies across fires, as shown in the reliability diagram (Fig. 5a). Most fires were variously slightly over- or under-predicted across classes, and none were consistently over- or under-predicted across all categories or by more than one class. The distributions of observed frequencies per predictive category per fire (Fig. 5a) demonstrate the amount of variability to expect in the probability of regeneration in a future fire. For example, at locations with a predicted probability of regeneration in the lowest category, one should expect regeneration levels between 1% and 28% most of the time although there is still a small chance that the probability could be as low as 0% and as high as 38%. Fig. 5b and Table 3 also show the range

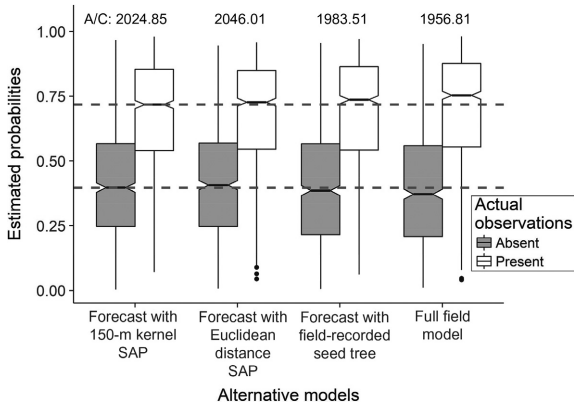

FIG. 4. Estimated model probabilities for four models, where the estimated probabilities of observing at least one conifer in a 60-m^2 area for each model are shown for plots where conifers were absent (gray boxes) and where they were present (white boxes). The forecast models differ by the variable representing seed availability: the kernel-based SAP with a 150-m neighborhood, Euclidean distance, and field-derived distance to seed tree. The full field model includes field-derived distance to seed tree as well as shrub cover, litter cover, and live tree basal area. Dashed lines show the median fitted values for the forecast model in comparison with all other models. The boxes define the first quartile (25th percentile) and third quartile (75th percentile), and the line within the box defines the median. The whiskers extend to the highest value that is within 1.5 times the interquartile range, and the dots are outliers that exceed this distance from the quartiles. The Akaike information criterion (AIC) for each model appear at the top of the graph.

of observed densities across all of the 24 fires used to build the forecast model, by the predicted probability class. For the same locations in the lowest category, one can expect a range of densities from 0 to 14,666 seedlings/ha, with a median value of 66. Forecasting the probability of observing at least one seedling in a 60-m^2 area at five years postfire across a "new" fire event (the 2014 King Fire) predicted ~33% of the fire area, or 12,975 hectares, in the two lowest probability classes (Fig. 5).

DISCUSSION

Continuous burn severity, the kernel-based SAP, and annual precipitation were the primary drivers of postfire conifer regeneration across the 24 fires we assessed. It was not surprising that precipitation was a major driver of regeneration patterns, since conifer seedlings are very sensitive to soil moisture (USDA Forest Service 1990), particularly in a Mediterranean climate. Snowpack can benefit Mediterranean climate ecosystems by providing a slow release of moisture in the spring and summer drought period. The weak negative trend in our model is likely related to a correlation with elevation, since our species of interest are generally found at lower elevations and may also be due to decreasing growing season length and reduced productivity at higher elevations. The negative effect of AET was initially surprising; since AET is usually considered a surrogate for productivity, we expected to see a positive relationship with regeneration probability. With more investigation, we found that the effect of AET varies somewhat with time since fire. On older fires (measured ≥5 yr postfire), regeneration probabilities declined with higher AET values (>450 mm), and

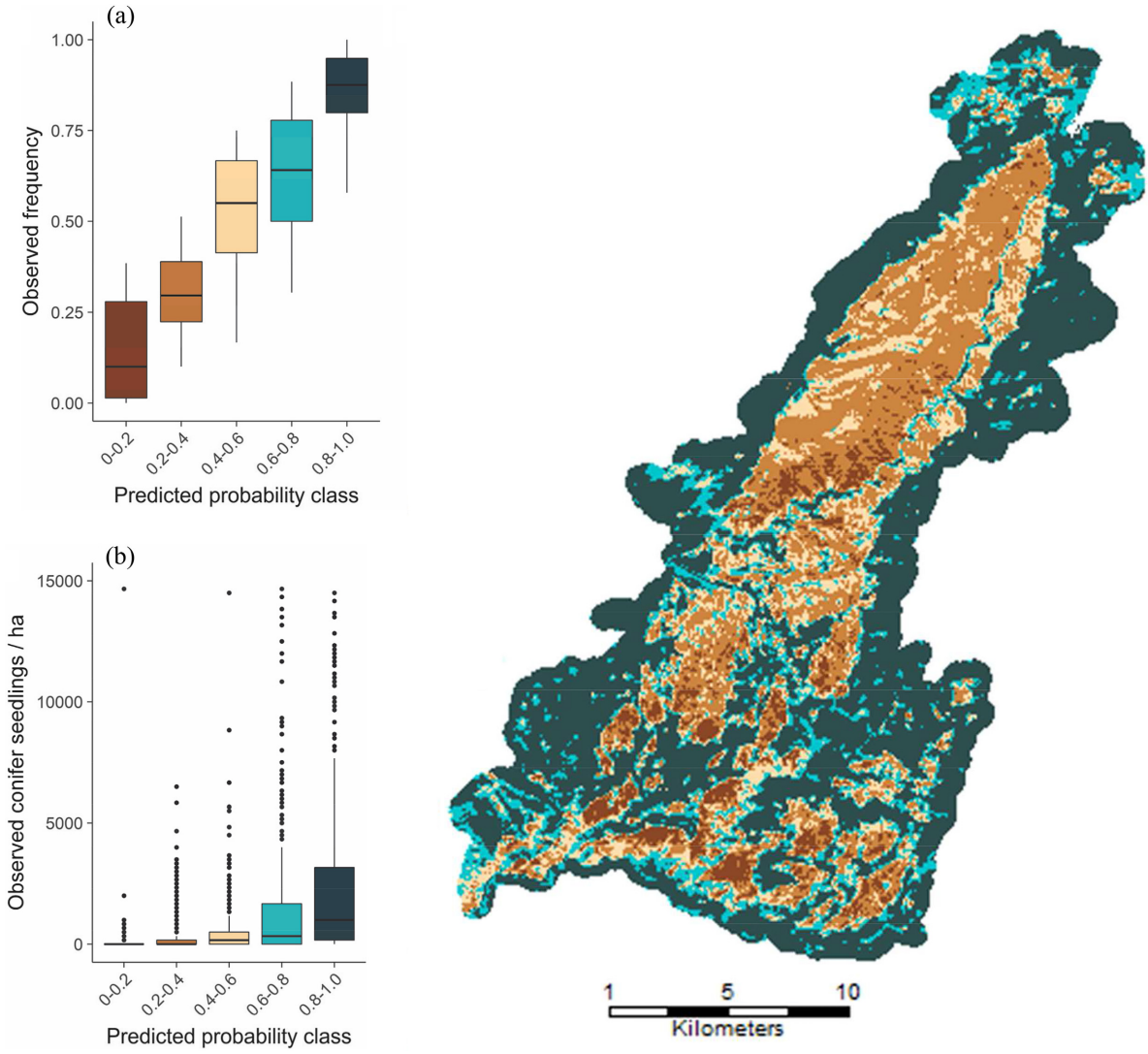

FIG. 5. Predictive map showing the probability of observing at least one regenerating conifer at the 60-m^2 (field plot) scale for the 2014 King Fire on the Eldorado National Forest. (a) The reliability diagram is created from the leave-one-out model validation procedure, where each fire is held out and predicted by the remaining 23 fires. The predictions are then binned into five classes, shown on the *x*-axis, and the actual frequency of conifer regeneration per fire within each class is plotted on the *y*-axis. (b) It shows the range of actual observed densities per fire across these same classes. Outliers exceeding 15,000 seedlings/ha were excluded for plot readability. For both, the boxes define the first quartile (25th percentile) and third quartile (75th percentile), and the line within the box defines the median. The whiskers extend to the highest value that is within 1.5 times the interquartile range, and the dots are outliers that exceed this distance from the quartiles.

TABLE 3. Minimum, maximum, median, mean, and standard error (SE) of observed conifer seedlings/ha for all 24 wildfires included in the forecast model by predicted probability class.

Predicted probability class	Observed densities (seedlings/ha)			
	Minimum	Maximum	Median	Mean (SE)
0.0–0.2	0	14,666	0	144 (86)
0.2–0.4	0	15,333	0	317 (55)
0.4–0.6	0	17,166	166	672 (101)
0.6–0.8	0	380,166	333	3,665 (985)
0.8–1.0	0	201,666	1,333	6,301 (755)

Notes: The model is at least one conifer. Seedlings were rounded down to whole number.

this trend was strongest on the oldest fires and as PPT increased. In contrast, on fires measured <5 yr postfire, there was a positive effect on regeneration probabilities at both moderate (300–450 mm) and high AET values. We hypothesize that the increased productivity associated with increasing AET is having a disproportionate, positive effect on competing vegetation (shrub, grass, hardwood). The longer the time since fire, the more the time for other vegetation to grow and become more competitive with conifer seedlings. Exploratory models of the relationship of shrub cover with AET were weak, but did support this hypothesis. Although competition from shrubs and sprouting trees may have less of an effect in some systems (Owen et al. 2017), it

is generally associated with reductions in conifer regeneration in the mixed conifer systems of California (Collins and Roller 2013, Welch et al. 2016, Safford and Stevens 2017, Tepley et al. 2017).

When scaling from the plot scale to the landscape scale in a forecasting framework, the kernel-based SAP did not perform as well as field-derived distance to seed tree but performed better than models with no spatial term or Euclidean distance. This suggests that the kernel-based SAPs are a reasonable proxy for neighborhood seed availability. The increased performance is likely due in part to the ability of the kernel-based SAPs to account for patch configuration and its neighborhood effect, rather than the more one-dimensional Euclidean distance. The 150-m neighborhood (or bandwidth) SAP is somewhat larger than the "rule of thumb" for dispersal in these systems, which holds that most seeds generally disperse within one to two tree heights of the parent tree (McDonald 1980); the tallest trees tend to be 40–50 m in these ecosystems. We speculate that there are likely several factors at work here. First, this rule of thumb does not incorporate long-distance seed dispersal, which is less common but likely important for regeneration patterns, especially for the pine species that have significant animal dispersal (Clark et al. 1999, Vander Wall 2008). Work elsewhere in the western United States has documented at least some regeneration at much greater distances from patch edges, for example up to 400 m in Ziegler et al. (2017) and Owen et al. (2017). In addition, the larger neighborhood may also be the result of lumping five species with a range of seed sizes: species such as white fir and incense-cedar produce lighter seeds that can travel notably farther than the heavier seeded pine species (Safford and Stevens 2017). In addition, as a proxy based on remote sensing, it is likely that there are live trees in areas that were not detected by LEMMA, many of which may occur near the edge of a high-severity patch that are contributing to the seed rain.

That distance to seed source is a major driver (and limitation) for postfire conifer regeneration patterns is echoed in other studies in similar systems (Greene and Johnson 2000, Bonnet et al. 2005, Franklin and Bergman 2011, Collins and Roller 2013, Dodson and Root 2013, Harvey et al. 2016, Kemp et al. 2016, Welch et al. 2016). Our documentation of these patterns is not novel, but it is unique in its scope (1,848 field plots in 24 wildfires throughout California) and in our explicit consideration of the neighborhood as a means to scale plot-level data to the landscape. Although one other study also used kernel-based methods to examine the importance of neighborhood characteristics (Haire and McGarigal 2010), our study develops a novel approach by creating a contiguous surface from these kernels that can be used to help predict regeneration across a new fire event.

An additional primary driver of regeneration probability was continuous burn severity (IA). Burn severity (IA) was correlated with the kernel-based SAP because the areas of highest burn severity are often far from live trees, which also results in lower potential seed availability. However, we retained burn severity in the model because we believe the severity of an individual pixel and potential for seed rain do represent different phenomena, despite their close relationship. The discrete values of RdNBR are important because even within a high-severity patch, pixels with lower burn severity values are more likely to have a live tree that survived the fire, which may not be detected in the SAP. Second, the satellite-derived measurements of burn severity may indirectly reflect other ecologically important metrics, including amount of fuel consumption and soil heating, which could have subsequent effects on the soil surface, underground processes, and microclimates that can affect regeneration (Miller and Thode 2007).

The predicted spatial patterns of regeneration at five years postfire on the King Fire suggest that patch configuration and size are critical for postfire conifer regeneration probabilities. Approximately one-third of the fire area (12,975 ha) is in the two lowest prediction classes, most of which occurs in the large contiguous patch of high severity that is more seed limited. Some research suggests that overstory recruitment occurs on decadal scales, so these patterns may change with time (Russell et al. 1998, Haire and McGarigal 2010). Haire and McGarigal (2010) have also shown that recolonization of the foundation tree species generally occurs in a wave-like front, where seedlings establish somewhat near parent trees, grow, and themselves disperse seeds further into patch interiors. Our spatially explicit forecast model suggests the same trend, where probabilities were higher nearer to the lesser burned edge. However, the applicability of these studies to modern fires is limited because they focused on much smaller patches of high severity than are occurring in more recent fires in the region, which can be thousands of hectares in size (e.g., the 2013 Rim Fire, 2014 King Fire). Maximum fire size in the study by Russell et al. (1998) was 100 ha, and the maximum individual high-severity patch size examined by Haire and McGarigal (2010) was 947 ha. In larger high-severity patches, regeneration via the wave-like front would likely require even longer timescales. During this time, the warming climate may compress the regeneration niche for the current conifer dominants, increasing the potential for type conversions (Feddema et al. 2013, Savage et al. 2013, Bell et al. 2014, Petrie et al. 2017). However, our understanding of the relationship between regeneration and climate drivers is limited (Petrie et al. 2016), and these relationships can be modified by other drivers (Dobrowski et al. 2015).

Because the low probabilities of regeneration are driven in part by proximity to seed sources, our results suggest that forest restoration treatments designed to reduce fuels, and in turn reduce fire severity and the size of individual high-severity patches, could affect postfire trajectories for stand development (Stephens et al. 2016). In addition to minimizing distance to seed source, such treatments could also buffer against drastic changes to the regeneration niche by retaining some forest canopy cover, which has an important moderating influence on realized climate at the soil surface and can increase seedling survival (Dobrowski et al. 2015).

It is important to note that within some areas with low regeneration probabilities, there are potentially areas that were not forested historically, because they are less suitable sites from the standpoint of precipitation or AET, or they may be sites that are physiographically prone to severe fire (windward, south- or west-facing upper slopes, for example). It is possible that these areas are only currently forested as a result of a century of fire exclusion, which enabled tree expansion into previously unsuitable habitats (Nagel and

Taylor 2005). For example, one of the smaller high-severity patches (~400 ha) at the southern end of the King Fire is primarily in the lowest probability class, because despite having relatively high seed input, the annual precipitation values at that location are very low. In general, areas where a lack of regeneration may not be of great concern could be inferred by annual precipitation and topographic position.

It is also important to consider what level of regeneration probability across these large patches is sufficient to restore historical forest densities that are likely more resilient to wildfire, pests, and the changing climate. For example, of the 18,272 ha that burned severely in the King Fire, 2,304 ha are in the lowest (0–20% probability) predicted class for observing at least one seedling per 60 m^2 and 9,199 ha are in the second lowest (20–40% probability) predicted class, most of which occurs in the large, interior high-severity patch (Fig. 5). Based on observed seedling densities in these classes, one can expect a variable response, with means at 144 ± 86 seedlings/ha in the lowest class and 317 ± 55 seedlings/ha in the second to lowest class (Table 3, Fig. 5b; mean ± SE). Median responses for both of these classes were 0 seedlings/ha, and the percentile distributions of the observed data show that one can expect 0 seedlings/ha for ~80% of the area in the lowest class (Table 3, Fig. 5b). Moreover, many of the seedlings observed in this study were fairly young, which also has implications for likelihood of reforestation, since young seedlings can suffer high mortality in the usually dry Mediterranean climate summer (Fowells and Stark 1965). Although the bud scar method we used is an imperfect measure of seedling age, it gives us a general idea about age structure (i.e., there may be some error in the age estimates, but it is unlikely that any of the seedlings recorded as three years old were actually first-year seedlings, for example). In the high-severity areas measured in this study, over 70% of the seedlings observed were ≤3 yr old. First-year seedling mortality is highly dependent on site conditions and species, where pines on favorable sites can have mortality rates as low as ~50%, but average mortality rates across species and sites can be as high as 80% (Fowells and Stark 1965). Mortality of first-year seedlings in high-severity areas may be even higher, since the study by Fowells and Stark (1965) used exclosures on all sites and managed competing vegetation on a subset of them. Another study that tracked seedlings through time found that mortality rates by year three can range from 57% to 70% of the initial seedling population (Fowells and Schubert 1951). Given the high percentage of young seedlings in the data set, it is likely that some of the regeneration predicted at five years postfire will not survive into the future. In addition, the model also shows significant decreases in regeneration probabilities on older fires, likely reflecting declines with increased shrub dominance. It is also important to recall that although the maps we produced capture some of the spatial variation in seedling response, because we binned the predictions into five classes, some of this variation is lost. The means are averaging over areas with very low probabilities (and subsequently, densities) that are far from residuals tree seed sources, and areas with slightly higher probabilities/densities that are closer to patch edges. Given the potential for mortality and decreases in density through time, the observed regeneration densities in these lower probability classes may not be adequate to create a forest that resembles historical forest densities, at least in some areas (Collins et al. 2011, Safford and Stevens 2017), or meet desired management conditions. However, more recruitment could occur through time, which could also be timed with conditions that promote greater survival (such as more favorable weather in the first few years postfire); in this case, even when accounting for probable mortality, the remaining seedling densities would be more likely to achieve historical densities. More research on recruitment trends through time in severely burned areas could better inform possible trajectories.

Forest managers using this tool for reforestation planning will also want to consider where seedling densities may be too high. In the King Fire, areas in the 80–100% category had an observed median density of 4,458 seedlings/ha, which is likely too high to create fire- or drought-resilient forests, even if there is notable seedling mortality over time (Lydersen et al. 2014, Young et al. 2017). Given that this class is located mostly in lower-severity areas that also have an intact overstory, seedling densities in these areas could result in overly dense forests that are highly susceptible to water stress, fire, and insect and disease outbreaks unless thinning disturbances are permitted to occur, such as regular fires or fire surrogates (e.g., mechanical or hand thinning).

Model limitations

There are numerous assumptions in our model as well as sources of uncertainty. First, the kernel-based SAPs were based on LEMMA map products, which are themselves modeled using FIA plots found at low density across the landscape (Ohmann et al. 2014). In addition, although we calculated annual seed production, this approach does not explicitly model seed dispersal. Although there is some disagreement on the best shape of a dispersal kernel, none have suggested using a Gaussian distribution, which we used here. The log-normal and a "fat-tailed" kernel are considered more accurate representations of seed dispersal (Clark et al. 1999, Greene and Johnson 2000), but these shapes are not readily available for kernel interpolations across a landscape in ArcMap. Sensitivity analyses on surfaces produced with the other available kernel shapes (Exponential, Quartic, Constant, Polynomial, Epanechnikov) showed little change in the models; this is likely due to our use of the kernel at each 30-m pixel, rather than centering the kernels on individual trees dispersing seeds. Stem mapping by species and size class would be required to truly map and predict seed dispersal, but this is likely too intensive to be practical at these scales since detailed stand structure data at the scale of an entire fire are generally lacking, and distinguishing species with publicly available remote sensing techniques is not sufficiently reliable at this point.

Another limitation of our model is our inability to predict temporal variations in postfire weather patterns and masting. The timing and occurrence of favorable weather conditions and mast-year seed production could have a substantial impact on regeneration patterns (Brown 2006, Keyes and González 2015, Rother and Veblen 2017). Although we could include postfire weather patterns for the fires studied here, we could not translate them into a forecasting framework because we cannot reliably predict annual weather patterns into the future. In addition,

masting patterns vary within species across their range, yet detailed data on mast years after the fires studied here are unavailable. Even if they were, it would also be difficult to predict masting into the future for a forecast model. Future work could create a suite of models that assumed favorable versus unfavorable conditions and variable masting patterns, to show a range of possible outcomes.

We also assume that lumping together conifer species with different shade, drought, and fire tolerances, which increased our sample size of actual observations, also probably muted some responses. For example, the best SAP scale for predicting regeneration may vary by species due to differences in seed size and morphology. Future work will examine the dominant conifer species separately and compare differences in response to the individual variables. We also lumped all age classes of observed regeneration; however, we know that mortality of first-year seedlings is particularly high and that prediction of established seedlings (perhaps >3 yr old) would give a better indication of future reforestation patterns and densities. We explored models predicting established seedlings, but they performed very poorly. We hypothesize this is because survival and establishment are likely more tied to localized competition and microsite characteristics, features that we are unable to model at the landscape scale.

Finally, this model should not be applied in regions outside of the mixed conifer forests of California, because the predictions are based on regional relationships between regeneration probability and predictors. However, the framework we used for modeling, including the creation of SAPs to represent seed availability, could be used to create models for non-serotinous forest types in other regions where robust regeneration data sets exist.

Management Applications

This spatially explicit predictive model can aid managers of non-serotinous yellow pine and mixed conifer forests in California and neighboring parts of the North American Mediterranean climate zone to predict where postfire regeneration five years after fire is likely to meet, or not meet, management target densities. Prediction maps such as the one shown in Fig. 5 can help identify areas where regeneration probabilities are lowest and can be used to prioritize limited resources for planting when managers decide to actively reforest an area. Because of the size of the sampling unit and presence/absence approach, the model predicts the probability of observing one conifer seedling, of any of the six focal species, in a 60-m^2 area. To translate that to something more meaningful for management decision making, managers can refer to Table 3 and Fig. 5b, which shows the range of observed seedling densities across fires within each probability class. The median values may be especially useful where land managers are relying on seedling stocking guidelines that require at least 50% of the area of interest exhibit regeneration (Welch et al. 2016). At the scale of the landscape, this model can help managers better anticipate variability for long-term planning.

Because there is always variability on the ground, we recommend that managers use this model in concert with the field tool and protocol developed by Welch et al. (2016). Their tool outlines field-observed characteristics that can be used to locally fine-tune the predictions from the forecast map generated by our study.

Conclusions

The spatially explicit model developed in this study highlights the variability in regeneration potential across a burned landscape. The probability of successful germination and regeneration is modified by climatic and topographic characteristics, but the most limiting factor for regeneration is the critical, initial biological filter of seed availability. We found that remote sensing-based proxies for seed source (burn severity and the kernel-based SAP) were reasonable approximations for field-derived seed sources measurements for modeling at the landscape scale.

The results of this modeling emphasize the importance of forest restoration treatments that can help limit high-severity patch size and increase forest resilience to wildfire (Fulé et al. 2012, Stephens et al. 2013). Predicted seedling densities from our modeling show that without management intervention, the largest high-severity patch in the King Fire could remain shrub dominated for an extended period. Where forest persistence is desired, restoration treatments in live forests that are designed to reduce high-severity patch sizes when fire does occur may be the most effective approach. In addition to maintaining forested conditions where desired, reducing individual patch sizes of high severity can promote habitat heterogeneity across the landscape, thereby benefitting a wider suite of species and ecosystem services (Turner 2010, North et al. 2012, Mallek et al. 2013, Turner et al. 2013).

Acknowledgments

This work was funded by a cost-share agreement between the USDA Forest Service, Pacific Southwest Region and the University of California, Berkeley. Work could not have been accomplished without the help of dozens of field technicians that collected the data for the 1,848 plots used in this study. Local National Forests in the Pacific Southwest Region provided extensive assistance with site access and fieldwork coordination.

Literature Cited

Avery, T. E., and H. E. Burkhard. 2015. Forest measurements. Fifth edition. Waveland Press, Long Grove, Illinois, USA.

Bell, D. M., J. B. Bradford, and W. K. Lauenroth. 2014. Early indicators of change: divergent climate envelopes between tree life stages imply range shifts in the western United States. Global Ecology and Biogeography 23:168–180.

Bonnet, V. H., A. W. Schoettle, and W. D. Shepperd. 2005. Postfire environmental conditions influence the spatial pattern of regeneration for *Pinus ponderosa*. Canadian Journal of Forest Research 35:37–47.

Brown, P. M. 2006. Climate effects on fire regimes and tree recruitment in Black Hills ponderosa pine forests. Ecology 87:2500–2510.

Chambers, M. E., P. J. Fornwalt, S. L. Malone, and M. Battaglia. 2016. Patterns of conifer regeneration following high severity wildfire in ponderosa pine-dominated forests of the Colorado Front Range. Forest Ecology and Management 378:57–67.

Clark, J. S., M. Silman, R. Kern, E. Macklin, and J. HilleRisLambers. 1999. Seed dispersal near and far: patterns across temperate and tropical forests. Ecology 80:1475–1494.

Collins, B. M., and G. B. Roller. 2013. Early forest dynamics in stand-replacing fire patches in the northern Sierra Nevada, California, USA. Landscape Ecology 28:1801–1813.

Collins, B. M., and S. L. Stephens. 2010. Stand-replacing patches within a "mixed severity" fire regime: quantitative characterization using recent fires in a long-established natural fire area. Landscape Ecology 25:927–939.

Collins, B. M., J. D. Miller, A. E. Thode, M. Kelly, J. W. van Wagtendonk, and S. L. Stephens. 2009. Interactions among wildland fires in a long-established Sierra Nevada natural fire area. Ecosystems 12:114–128.

Collins, B. M., R. G. Everett, and S. L. Stephens. 2011. Impacts of fire exclusion and recent managed fire on forest structure in old growth Sierra Nevada mixed-conifer forests. Ecosphere 2:art51.

Collins, B. M., J. T. Stevens, J. D. Miller, S. L. Stephens, P. M. Brown, and M. P. North. 2017. Alternative characterization of forest fire regimes: incorporating spatial patterns. Landscape Ecology 32:1543–1552.

Coppoletta, M., K. E. Merriam, and B. M. Collins. 2016. Post-fire vegetation and fuel development influences fire severity patterns in reburns. Ecological Applications 26:686–699.

Crotteau, J. S., J. Morgan Varner III, and M. W. Ritchie. 2013. Post-fire regeneration across a fire severity gradient in the southern Cascades. Forest Ecology and Management 287:103–112.

Daly, C., and D. Shankman. 1985. Seedling establishment by conifers above tree limit on Niwot Ridge, Front Range, Colorado, USA. Arctic and Alpine Research 17:389–400.

DeSiervo, M. H., E. S. Jules, and H. D. Safford. 2015. Disturbance response across a productivity gradient: postfire vegetation in serpentine and nonserpentine forests. Ecosphere 6:1–19.

Dobrowski, S. Z., A. K. Swanson, J. T. Abatzoglou, Z. A. Holden, H. D. Safford, M. K. Schwartz, and D. G. Gavin. 2015. Forest structure and species traits mediate projected recruitment declines in western US tree species: Tree recruitment patterns in the western US. Global Ecology and Biogeography 24:917–927.

Dodson, E. K., and H. T. Root. 2013. Conifer regeneration following stand-replacing wildfire varies along an elevation gradient in a ponderosa pine forest, Oregon, USA. Forest Ecology and Management 302:163–170.

Donato, D. C., B. J. Harvey, and M. G. Turner. 2016. Regeneration of montane forests 24 years after the 1988 Yellowstone fires: A fire-catalyzed shift in lower treelines? Ecosphere 7:e01410.

Feddema, J. J., J. N. Mast, and M. Savage. 2013. Modeling high-severity fire, drought and climate change impacts on ponderosa pine regeneration. Ecological Modelling 253:56–69.

Flint, L., A. Flint, J. H. Thorne, and R. Boynton. 2013. Fine-scale hydrologic modeling for regional landscape applications: the California Basin Characterization Model development and performance. Ecological Processes 2:1–21.

Fowells, H. A., and G. H. Schubert. 1951. Natural reproduction in certain cutover pine-fir stands in California. Journal of Forestry 49:192–196.

Fowells, H. A., and N. B. Stark. 1965. Natural regeneration in relation to environment in the mixed conifer forest type of California. Research Paper PSW-RP-24. Pacific Southwest Forest and Range Experiment Station, U.S. Department of Agriculture Forest Service, Berkeley, California, USA.

Franklin, J. F. 1974. Abies. Pages 168–183 *in* C. S. Schopmeyer, editor. Seeds of woody plants in the United States. U.S. Department of Agriculture Forest Service, Washington, District of Columbia, USA.

Franklin, J., and E. Bergman. 2011. Patterns of pine regeneration following a large, severe wildfire in the mountains of southern California. Canadian Journal of Forest Research 41:810–821.

Fulé, P. Z., J. E. Crouse, J. P. Roccaforte, and E. L. Kalies. 2012. Do thinning and/or burning treatments in western USA ponderosa or Jeffrey pine-dominated forests help restore natural fire behavior? Forest Ecology and Management 269:68–81.

Gray, A. N., H. S. J. Zald, R. A. Kern, and M. North. 2005. Stand conditions associated with tree regeneration in Sierran mixed-conifer forests. Forest Science 51:198–210.

Greene, D. F., and E. A. Johnson. 1994. Estimating the mean annual seed production of trees. Ecology 75:642–647.

Greene, D. F., and E. A. Johnson. 2000. Tree recruitment from burn edges. Canadian Journal of Forest Research 30:1264–1274.

Haire, S. L., and K. McGarigal. 2010. Effects of landscape patterns of fire severity on regenerating ponderosa pine forests (*Pinus ponderosa*) in New Mexico and Arizona, USA. Landscape Ecology 25:1055–1069.

Harvey, B. J., D. C. Donato, and M. G. Turner. 2016. High and dry: post-fire tree seedling establishment in subalpine forests decreases with post-fire drought and large stand-replacing burn patches: Drought and post-fire tree seedlings. Global Ecology and Biogeography 25:655–669.

Hastie, T., R. Tibshirani, and J. Friedman. 2001. The elements of statistical learning. Data mining, inference, and prediction. Springer-Verlag, New York, New York, USA.

Kemp, K. B., P. E. Higuera, and P. Morgan. 2016. Fire legacies impact conifer regeneration across environmental gradients in the U.S. northern Rockies. Landscape Ecology 31:619–636.

Keyes, C. R., and R. M. González. 2015. Climate-influenced ponderosa pine (*Pinus ponderosa*) seed masting trends in western Montana, USA. Forest Systems 24:021.

Keyes, C. R., D. A. Maguire, and J. C. Tappeiner. 2009. Recruitment of ponderosa pine seedlings in the Cascade Range. Forest Ecology and Management 257:495–501.

Krugman, S. L., and J. L. Jenkinson. 1974. Pinus. Pages 598–638 *in* C. S. Schopmeyer, editor. Seeds of woody plants in the United States. U.S. Department of Agriculture Forest Service, Washington, District of Columbia, USA.

Lydersen, J. M., M. P. North, and B. M. Collins. 2014. Severity of an uncharacteristically large wildfire, the Rim Fire, in forests with relatively restored frequent fire regimes. Forest Ecology and Management 328:326–334.

Lydersen, J. M., B. M. Collins, J. D. Miller, D. L. Fry, and S. L. Stephens. 2016. Relating fire-caused change in forest structure to remotely sensed estimates of fire severity. Fire Ecology 12:99–116.

Mallek, C., H. D. Safford, J. Viers, and J. Miller. 2013. Modern departures in fire severity and area by forest type, Sierra Nevada and southern Cascades, California, USA. Ecosphere 4:1–28.

McDonald, P. M. 1980. Seed dissemination in small clearcuttings in north-central California. US Department of Agriculture, Forest Service, Pacific Southwest Forest and Range Experiment Station, Research Paper, PSW-150.

Millar, C. I., R. D. Westfall, D. L. Delaney, J. C. King, and L. J. Graumlich. 2004. Response of subalpine conifers in the Sierra Nevada, California, USA, to 20th-century warming and decadal climate variability. Arctic, Antarctic, and Alpine Research 36:181–200.

Miller, J. D., E. E. Knapp, C. H. Key, C. N. Skinner, C. J. Isbell, R. M. Creasy, and J. W. Sherlock. 2009. Calibration and validation of the relative differenced Normalized Burn Ratio (RdNBR) to three measures of fire severity in the Sierra Nevada and Klamath Mountains, California, USA. Remote Sensing of Environment 113:645–656.

Miller, J. D., and H. Safford. 2012. Trends in wildfire severity: 1984 to 2010 in the Sierra Nevada, Modoc Plateau, and Southern Cascades, California, USA. Fire Ecology 8:41–57.

Miller, J. D., and A. E. Thode. 2007. Quantifying burn severity in a heterogeneous landscape with a relative version of the delta Normalized Burn Ratio (dNBR). Remote Sensing of Environment 109:66–80.

Miller, J. D., C. N. Skinner, H. D. Safford, E. E. Knapp, and C. M. Ramirez. 2012. Trends and causes of severity, size, and number of fires in northwestern California, USA. Ecological Applications 22:184–203.

Nagel, T. A., and A. H. Taylor. 2005. Fire and persistence of montane chaparral in mixed conifer forest landscapes in the northern Sierra Nevada, Lake Tahoe Basin, California, USA. Journal of the Torrey Botanical Society 132:442–457.

North, M., P. Stine, K. O'Hara, W. Zielinski, and S. Stephens. 2012. An ecosystem management strategy for Sierran mixed-conifer

forests. Second printing with addendum. General Technical Report. USDA Forest Service, Pacific Southwest Research Station, Albany, California, USA.

Ohlmann, J. L., and M. J. Gregory. 2002. Predictive mapping of forest composition and structure with direct gradient analysis and nearest neighbor imputation in coastal Oregon, U.S.A. Canadian Journal of Forest Research 32:725–741.

Ohmann, J., M. Gregory, and H. Roberts. 2014. GNN Accuracy Assessment Report California Sierra Nevada (Modeling Region 232). Model type: basal-area by species-size combinations. Page 26. Oregon State University and USFS Pacific Northwest Research Station.

Owen, S. M., C. H. Sieg, A. J. Sánchez Meador, P. Z. Fulé, J. M. Iniguez, L. S. Baggett, P. J. Fornwalt, and M. A. Battaglia. 2017. Spatial patterns of ponderosa pine regeneration in high-severity burn patches. Forest Ecology and Management 405:134–149.

Owston, P. W., and W. I. Stein. 1974. Pseudotsuga. Pages 674–683 *in* C. S. Schopmeyer, editor. Seeds of woody plants in the United States. U.S. Department of Agriculture Forest Service, Washington, District of Columbia, USA.

Parsons, D. J., and S. H. DeBenedetti. 1979. Impact of fire suppression on a mixed-conifer forest. Forest Ecology and Management 2:21–33.

Perry, D. A., P. F. Hessburg, C. N. Skinner, T. A. Spies, S. L. Stephens, A. H. Taylor, J. F. Franklin, B. McComb, and G. Riegel. 2011. The ecology of mixed severity fire regimes in Washington, Oregon, and Northern California. Forest Ecology and Management 262:703–717.

Petrie, M. D., A. M. Wildeman, J. B. Bradford, R. M. Hubbard, and W. K. Lauenroth. 2016. A review of precipitation and temperature control on seedling emergence and establishment for ponderosa and lodgepole pine forest regeneration. Forest Ecology and Management 361:328–338.

Petrie, M. D., J. B. Bradford, R. M. Hubbard, W. K. Lauenroth, C. M. Andrews, and D. R. Schlaepfer. 2017. Climate change may restrict dryland forest regeneration in the 21st century. Ecology 98:1548–1559.

Puhlick, J. J., D. C. Laughlin, and M. M. Moore. 2012. Factors influencing ponderosa pine regeneration in the southwestern USA. Forest Ecology and Management 264:10–19.

Rother, M. T., and T. T. Veblen. 2017. Climate drives episodic conifer establishment after fire in dry ponderosa pine forests of the Colorado Front Range, USA. Forests 8:159.

Russell, W. H., J. McBride, and R. Rowntree. 1998. Revegetation after four stand-replacing fires in the Lake Tahoe Basin. Madroño 45:40–46.

Safford, H. D., and J. T. Stevens. 2017. Natural range of variation (NRV) for yellow pine and mixed conifer forests in the Sierra Nevada, southern Cascades, and Modoc and Inyo National Forests, California, USA. General Technical Report. USDA Forest Service, Pacific Southwest Research Station, Albany, California, USA.

Savage, M., J. N. Mast, and J. J. Feddema. 2013. Double whammy: high-severity fire and drought in ponderosa pine forests of the Southwest. Canadian Journal of Forest Research 43:570–583.

Shive, K. L., B. L. Estes, A. M. White, H. D. Safford, K. L. O'Hara, and S. L. Stephens. 2017. Rice straw mulch for post-fire erosion control: assessing non-target effects on vegetation communities. International Journal of Wildland Fire 26:538–549.

Stein, W. I. 1974. Libocedrus. Pages 494–499 *in* C. S. Schopmeyer, editor. Seeds of woody plants in the United States. U.S. Department of Agriculture Forest Service, Washington, District of Columbia, USA.

Stephens, S. L., and B. M. Collins. 2004. Fire regimes of mixed conifer forests in the north-central Sierra Nevada at multiple spatial scales. Northwest Science 78:12–23.

Stephens, S. L., and L. W. Ruth. 2005. Federal forest policy in the United States. Ecological Applications 15:532–542.

Stephens, S. L., J. K. Agee, P. Z. Fule, M. P. North, W. H. Romme, T. W. Swetnam, and M. G. Turner. 2013. Managing forests and fire in changing climates. Science 342:41–42.

Stephens, S. L., B. M. Collins, E. Biber, and P. Z. Fulé. 2016. U.S. federal fire and forest policy: emphasizing resilience in dry forests. Ecosphere 7:e01584.

Stevens, J. T., B. M. Collins, J. D. Miller, M. P. North, and S. L. Stephens. 2017. Changing spatial patterns of stand-replacing fire in California conifer forests. Forest Ecology and Management 406:28–36.

Sugihara, N. G., J. van Wagtendonk, J. Fites-Kaufman, A. E. Thode, and J. K. Agee, editors. 2006. Fire in California's ecosystems. University of California Press, Oakland, California.

Tepley, A., J. Thompson, H. Epstein, and K. Anderson-Teixeira. 2017. Vulnerability to forest loss through altered postfire recovery dynamics in a warming climate in the Klamath Mountains. Global Change Biology 23:4117–4132.

Turner, M. G. 1989. Landscape ecology: the effect of pattern on process. Annual Review of Ecology and Systematics 20:171–197.

Turner, M. G. 2010. Disturbance and landscape dynamics in a changing world. Ecology 91:2833–2849.

Turner, M. G., W. H. Romme, R. H. Gardner, and W. W. Hargrove. 1997. Effects of fire size and pattern on early succession in Yellowstone National Park. Ecological Monographs 67:411–433.

Turner, M. G., D. C. Donato, and W. H. Romme. 2013. Consequences of spatial heterogeneity for ecosystem services in changing forest landscapes: priorities for future research. Landscape Ecology 28:1081–1097.

Urza, A. K., and J. S. Sibold. 2013. Nondestructive aging of postfire seedlings for four conifer species in northwestern Montana. Western Journal of Applied Forestry 28:22–29.

U.S. Geological Survey. 2014. U.S. Geological Survey, The National Map. http://nationalmap.gov/3dep_prodserv.html

USDA Forest Service. 1990. Silvics of North America volume 1: conifers. United States Department of Agriculture (USDA), Forest Service, Agriculture Handbook 654.

Vander Wall, S. B. 2008. On the relative contributions of wind vs. animals to seed dispersal of four Sierra Nevada pines. Ecology 89:1837–1849.

Venable, D. L. 1992. Size-number trade-offs and the variation of seed size with plant resource status. American Naturalist 140:287–304.

Welch, K. R., H. D. Safford, and T. P. Young. 2016. Predicting conifer establishment post wildfire in mixed conifer forests of the North American Mediterranean-climate zone. Ecosphere 7:e01609.

Westerling, A. L., H. G. Hidalgo, D. R. Cayan, and T. W. Swetnam. 2006. Warming and earlier spring increase western US forest wildfire activity. Science 313:940–943.

Wood, S. N. 2006. Generalized additive models: an introduction with R. Chapman and Hall/CRC Press, Boca Raton, Florida.

Young, D. J. N., J. T. Stevens, J. M. Earles, J. Moore, A. Ellis, A. L. Jirka, and A. M. Latimer. 2017. Long-term climate and competition explain forest mortality patterns under extreme drought. Ecology Letters 20:78–86.

Ziegler, J., C. Hoffman, P. Fornwalt, C. Sieg, M. Battaglia, M. Chambers, and J. Iniguez. 2017. Tree regeneration spatial patterns in ponderosa pine forests following stand-replacing fire: influence of topography and neighbors. Forests 8:391.

Data Availability

Data are available from the FRAMES Resource Catalog: https://www.frames.gov/catalog/55902.